Monthly Notices
of the
ROYAL ASTRONOMICAL SOCIETY

MNRAS **430,** 638–651 (2013) doi:10.1093/mnras/sts675

Effect of the interactions and environment on nuclear activity

J. Sabater,[1,2]★ P. N. Best[1] and M. Argudo-Fernández[2]

[1]*Institute for Astronomy (IfA), University of Edinburgh, Royal Observatory, Blackford Hill, Edinburgh EH9 3HJ, UK*
[2]*Instituto de Astrofísica de Andalucía, CSIC, Apdo. 3004, E-18080 Granada, Spain*

Accepted 2012 December 18. Received 2012 December 18; in original form 2012 November 12

ABSTRACT

We present a study of the prevalence of optical and radio nuclear activity with respect to the environment and interactions in a sample of the Sloan Digital Sky Survey (SDSS) galaxies. The aim is to determine the independent effects of distinct aspects of source environment on the triggering of different types of nuclear activity. We defined a local density parameter and a tidal force estimator and used a cluster richness estimator from the literature to trace different aspects of environment and interaction. The possible correlations between the environmental parameters were removed using a principal component analysis. By far, the strongest trend found for the active galactic nuclei (AGN) fractions, of all AGN types, is with galaxy mass. We therefore applied a stratified statistical method that takes into account the effect of possible confounding factors like the galaxy mass. We found that (at fixed mass) the prevalence of optical AGN is a factor of 2–3 lower in the densest environments, but increases by a factor of $\sim$2 in the presence of strong one-on-one interactions. These effects are even more pronounced for star-forming nuclei. The importance of galaxy interactions decreases from star-forming nuclei to Seyferts to low-ionization nuclear emission-line regions to passive galaxies, in accordance with previous suggestions of an evolutionary time-sequence. The fraction of radio AGN increases very strongly (by nearly an order of magnitude) towards denser environments, and is also enhanced by galaxy interactions. Overall, the results agree with a scenario in which the mechanisms of accretion into the black hole are determined by the presence and nature of a supply of gas, which in turn is controlled by the local density of galaxies and their interactions. A plentiful cold gas supply is required to trigger star formation, optical AGN and radiatively efficient radio AGN. This is less common in the cold-gas-poor environments of groups and clusters, but is enhanced by one-on-one interactions which result in the flow of gas into nuclear regions; these two factors compete against each other. In the denser environments where cold gas is rare, cooling hot gas can supply the nucleus at a sufficient rate to fuel low-luminosity radiatively inefficient radio AGN. However, the increased prevalence of these AGN in interacting galaxies suggests that this is not the only mechanism by which radiatively inefficient AGN can be triggered.

Key words: catalogues – galaxies: active – galaxies: evolution – galaxies: interactions – radio continuum: galaxies.

1 INTRODUCTION

Active galactic nuclei (AGN) are closely related to galaxy formation and evolution. The black holes that power AGN are found in all massive galaxies and their masses are tightly correlated with both the masses and the velocity dispersions of the stellar bulges (e.g. Ferrarese & Merritt 2000; Gebhardt et al. 2000; Marconi & Hunt 2003). AGN may play an important role in the feedback mechanisms that control the growth of massive galaxies (see review by Cattaneo et al. 2009, and references therein). Interaction between galaxies can drive gas into the central region of the galaxy and trigger the AGN (Shlosman, Begelman & Frank 1990; Barnes & Hernquist 1991; Haan et al. 2009; Liu et al. 2011). However, a high fraction of AGN may by fuelled by secular processes (e.g. Silverman et al. 2011; Sabater et al. 2012).

The effect of the large-scale environment and of galaxy interactions on the triggering of an AGN has previously been studied by many authors, but contradictory results have been found. Quasars are thought to be associated with galaxy interactions (Sanders et al.

★ E-mail: jsm@roe.ac.uk

1988; Urrutia, Lacy & Becker 2008; Letawe, Letawe & Magain 2010) or a higher number of companions (Hutchings & Campbell 1983; Bahcall et al. 1997; Serber et al. 2006). Several studies found a direct relation between interaction and the presence of an optical AGN (Petrosian 1982; Koulouridis et al. 2006; Alonso et al. 2007; Rogers et al. 2009; Ellison et al. 2011; Hwang et al. 2012; Liu, Shen & Strauss 2012). On the other hand, other studies did not find this relation (Bushouse 1986; Schmitt 2001; Ellison et al. 2008; Li et al. 2008; Darg et al. 2010; Slavcheva-Mihova & Mihov 2011). In some cases, a lower prevalence of AGN is found in environments with higher density of galaxies (Carter et al. 2001; Miller et al. 2003; Kauffmann et al. 2004), or the AGN prevalence is found to depend upon distance to the centre of the nearest group or cluster (von der Linden et al. 2010). In contrast, Alonso, Coldwell & Garcia Lambas (2012) found an increase of the fraction of powerful AGN towards denser environments in sample face-on spiral galaxies. Some studies find signatures of mergers in active galaxies (Comerford et al. 2009; Smirnova, Moiseev & Afanasiev 2010; Villar-Martín et al. 2011, 2012), but, Grogin et al. (2005) found no connection between recent galaxy mergers and AGN. Making use of radio observations, Kuo et al. (2008) and Tang et al. (2008) measured the disruption of the atomic gas distribution and kinematics to trace interactions and found a clear relation with the presence of an AGN.

With respect to X-ray selected AGN, a higher incidence of signs of disruption in AGN (Koss et al. 2010) and a higher fraction of AGN in pairs (Silverman et al. 2011) and in the centre of clusters (Ruderman & Ebeling 2005) have been found. However, a relation between interaction and AGN was not found by Pierce et al. (2007), Georgakakis et al. (2009) or Gabor et al. (2009). Waskett et al. (2005) found that the environments of AGN are indistinguishable from those of normal, inactive galaxies. Finally, Silverman et al. (2009) found no difference between the fraction of AGN in groups and in field galaxies.

If radio-selected AGN are considered, Best et al. (2005a) found a tendency for radio-loud AGN to be located in richer environments. Reviglio & Helfand (2006) confirmed this trend for radio AGN, which is in contrast to that widely found for optical AGN. Brightest group and cluster galaxies are more likely to host a radio-loud AGN than other galaxies with similar stellar masses (e.g. Best et al. 2007). Domingue, Sulentic & Durbala (2005) found an excess of radio AGN in pairs of galaxies while no radio AGN were found in isolated galaxies (Sabater et al. 2008, 2010). While Heckman et al. (1986) found many radio AGN to be 'strongly peculiar' in optical morphology, Tal et al. (2009) found no correlation between radio AGN and tidal distortions. Nevertheless, there is recent evidence of the triggering of powerful radio galaxies by interactions (Bessiere et al. 2012; Ramos Almeida et al. 2012).

Part of the confusion from the results discussed above may involve the different definitions of 'environment' and 'interaction' used in the previous studies. This may be (a) a higher local density of neighbours, (b) the membership of a cluster or group versus field or filaments, (c) relative location within a group or cluster, or (d) one-on-one interactions. These definitions can lead to contradictory results since they trace different aspects of interaction and environment. It is known that many interacting galaxy pairs can be found in low-density regions (even void; Verley et al. 2007; Argudo-Fernández et al., in preparation), consequently, the concept 'field' is not equivalent to 'isolated'. We might expect the amount and physical conditions of the gas in galaxies that is used to fuel the AGN to be related to large-scale environment (e.g. Sijacki et al. 2007). On the other hand, interactions at the one-on-one level are expected to set the gravitational disturbances that could trigger the AGN. Therefore, it is fundamental to separate those different aspects when studying their effect on nuclear activity.

A further complication is the type, and luminosity, of the AGN selected in different studies. Although the emission of an AGN spans a wide range of the electromagnetic spectrum (Elvis et al. 1994), the different methods and wavelengths used to select AGN will also lead to the selection of different kinds of AGN. All of the selection methods are affected by selection effects (Ho 2008), for example, X-rays have been used to detect AGN that did not present optical emission lines (Martini et al. 2002). Selection based on optical emission lines can discern between Seyfert and low-ionization nuclear emission-line region (LINER; Heckman 1980) types; however, the final classification may depend on the exact processing method used and the classification criteria applied (e.g. Constantin & Vogeley 2006; Kewley et al. 2006). Best et al. (2005a) found that the probability of galaxy harbouring a radio AGN is independent of its optical classification and conclude that low-luminosity radio AGN and emission-line AGN are powered by different physical processes. Two main feeding mechanisms can be found in AGN: (a) 'standard' high-excitation radiatively efficient mode, and, (b) low-excitation radiatively inefficient mode (see Best & Heckman 2012, and references therein). Radiatively efficient AGN include luminous radio AGN (also called High Excitation Radio Galaxies or HERG) and the optical or X-ray AGN while radiatively inefficient ones are observed as low-luminosity radio AGN (Low Excitation Radio Galaxies or LERG; Hardcastle, Evans & Croston 2007). These types of feeding mechanisms can evolve in time (Hlavacek-Larrondo et al. 2012) and may be fundamental to explain the decline of star formation in large elliptical galaxies (Cattaneo et al. 2009).

It is also important to consider that many properties of galaxies depend on the environment, with clusters typically hosting more massive and more early-type galaxies than the field (e.g. Blanton & Moustakas 2009; Deng, He & Wen 2009; Park & Choi 2009; Deng, Chen & Jiang 2011). If samples are not well-matched (as has been the case for many previous studies) then these differences can give rise to false dependencies. In particular, it is known that galaxy mass is one of the most (if not *the* most) important driving factors for the prevalence of (a) optical (e.g. Kauffmann et al. 2003b), (b) radio (Best et al. 2005a) and (c) X-ray (Silverman et al. 2009; Tasse, Röttgering & Best 2011) selected AGN. The prevalence of AGN also depends upon galaxy morphology (Moles, Marquez & Perez 1995; Schawinski et al. 2010; Sabater et al. 2012). These properties are also closely related to the environment via the density–morphology and density–luminosity relations (Dressler 1980; Kauffmann et al. 2004; Blanton et al. 2005a; Deng et al. 2009, 2011; Park & Choi 2009). Indeed, Park & Choi (2009) suggest that galaxy properties are mainly driven by mass and morphology, and environment plays only a secondary role. Hence, these confounding factors should be carefully taken into account in order to obtain unbiased results.

We aim to study independently the effects of the large-scale environment and the smaller-scale interactions on the triggering of both radio and optically selected AGN. In Section 2, the sample and the data used are presented. We define a set of parameters to quantify the environment and the interactions that affect our galaxies, and these are described in Section 3. The results of the statistical studies that estimate the relation between the environment and interaction with the prevalence of different types of active nuclei are presented in Section 4. Finally, these results are discussed in Section 5 and the final conclusions are presented Section 6. Throughout the paper, the

following cosmological parameters are assumed: $\Omega_{\rm m} = 0.3$, $\Omega_\Lambda = 0.7$ and $H_0 = 70\,{\rm km\,s^{-1}\,Mpc^{-1}}$.

2 THE SAMPLE AND THE DATA

2.1 The sample

The sample was based on the seventh data release (DR7; Abazajian et al. 2009) of the Sloan Digital Sky Survey (SDSS; York et al. 2000). The base sample is composed of galaxies from the main spectroscopic sample (magnitudes between $14.5 < r < 17.77$; Strauss et al. 2002) with a redshift between 0.03 and 0.1. Galaxies with a redshift below 0.03 were discarded (a) to limit the search for companions to a reasonable area of the sky around the target galaxies, (b) to lessen the possible effect of the incompleteness of galaxies with high brightness and (c) to avoid the possible errors in the measurements of the photometry due to the large size of the galaxies. Galaxies with a redshift above 0.1 were also discarded (a) to allow a good signal-to-noise ratio for the emission lines used for the optical activity classification and for the radio-continuum emission used in the radio activity classification, and (b) to maximize the number of companions with similar luminosities that are covered by the spectroscopic survey. The evolutionary time between redshift 0.03 and 0.1 is $\approx 9 \times 10^8$ yr. We take no account of any evolution of the nuclear activity prevalence during this period, but this is supposed to be small and in any case any evolutionary effects are minimized by the use of the stratified statistical study. The sample is composed of galaxies from the table `Galaxy` which have an assigned spectroscopic object `specObjID` with a spectroscopic redshift (field `bsz`) within the limits.

A small percentage of luminous galaxies are not included in the main spectroscopic survey at lower redshifts (those with $r < 14.5$ which at $z = 0.03$ corresponds to $L_r \sim 10^{10.2}\,{\rm L}_\odot$). At $z = 0.1$ the magnitude limit corresponds to a luminosity limit in r band of $\sim 10^{9.4}\,{\rm L}_\odot$. For most of our analyses, stellar mass (see the next section) limits of $10 \leq \log(M/{\rm M}_\odot) \leq 12$ were applied to reduce the incompleteness. In any case, in our study we compute relative fractions of galaxies instead of absolute numbers. These fractions should not be biased by the small number of missing galaxies, especially since we observe no significant trends of any of the AGN fractions with redshift across our samples. The use of relative fractions, the cut in masses and the use of stratified statistical methods that take into account the mass of galaxies should mitigate the possible effect of the incompleteness.

The environmental parameters that we aimed to obtain could be affected if the target galaxy is close to the border of the SDSS footprint or near to a bright star. The potential loss of a significant fraction of companion galaxies could then cause an underestimation of the parameters. Hence, we discarded from our study galaxies that could be affected by these problems. To do this we used the New York University (NYU) Value-Added Galaxy Catalog (Blanton et al. 2005b), which provides additional data to the SDSS sample. The parameter `NEXPECT` found in the `simpleden` table gives an estimation of the number of tracer galaxies that can be found within a given fixed radius of a target galaxy. These tracer galaxies are homogeneously and randomly distributed but only within the coverage region of the SDSS spectroscopic survey. Hence, if the number is lower than a given value, it indicates that the region around the target galaxy is not completely covered by the survey. We discarded galaxies with `NEXPECT` < 0.45. In some cases, there were no available data from the NYU catalogue and we took the value of `NEXPECT` from the closest galaxy with data within a maximum of 30 arcmin radius. A visual inspection (using the software TOPCAT; Taylor 2005) showed that this process was reliable for the selection of galaxies in well-sampled SDSS areas. Four galaxies were manually added and three regions close to the borders (126 galaxies in total) were manually discarded. Two additional regions containing 1594 galaxies close to the borders were flagged later after finding systematic offsets for those galaxies in one of the environmental parameters that we computed (the tidal estimator; Section 3.2).

The final sample was composed of 267 977 galaxies. Reliable estimations of the cluster richness using a friends-of-friends (FoF) algorithm (as explained in Section 3.3) could only be obtained for galaxies brighter than $M_r - 5\log({\rm h}) = -20$. These galaxies constitute the *reduced sample* which was used when the cluster richness parameter was needed for the analysis. The total number of galaxies in each sample is shown in Table 1.

Table 1. Number of galaxies of each type.

Type[a]	Whole sample	Reduced sample	Whole sample M lim.[b]	Reduced sample M lim.
Total	267 977	107 176	201 425	106 503
Passive	99 180	47 333	90 174	47 311
Optical AGN	57 955	34 266	55 864	34 255
LINER	16 288	12 315	16 144	12 313
Seyfert	7170	3691	6763	3689
TO	34 497	18 260	32 957	18 253
SFN	110 842	25 577	55 387	24 937
Radio AGN	1137	1015	1129	1015
LERG	1087	979	1082	979
HERG	47	34	44	34

[a]Meaning of the different types: passive – galaxies with $L_{[\rm O\,III]} < 10^{6.5}\,{\rm L}_\odot$; optical AGN – galaxies with $L_{[\rm O\,III]} \geq 10^{6.5}\,{\rm L}_\odot$ classified as LINER, Seyferts or transition objects (TO); SFN – star-forming nuclei galaxies with $L_{[\rm O\,III]} \geq 10^{6.5}\,{\rm L}_\odot$; radio AGN – galaxies with $L_{1.4\,\rm GHz} \geq 10^{23}\,{\rm W\,m^{-2}\,Hz^{-1}}$ classified as radio AGN including HERG and LERG.
[b]Mass limited to $10 \leq \log(M/{\rm M}_\odot) \leq 12$.

2.2 AGN classification

Our aim was to check the dependence of the different nuclear activity types on the environment and interaction. For this study, we considered optically and radio selected nuclear activity types.

Data based on optical spectra were drawn from the Max Plank Institute for Astrophysics and Johns Hopkins University (MPA-JHU) added value spectroscopic catalogue (cf. Brinchmann et al. 2004). Information about total stellar mass (Kauffmann et al. 2003a) and the classification of the optical nuclear activity based on the accurate measurement of emission-line fluxes can be found in this catalogue. The classification of optical activity is based on the typical diagnostic diagrams (BPT diagrams; Baldwin, Phillips & Terlevich 1981; Kauffmann et al. 2003b). The following optically selected nuclear activity types are distinguished: (a) star-forming nuclei (SFN); (b) transition objects (TO; which may contain a mix of star formation and an AGN); (c) Seyfert, (d) LINER and (e) passive galaxies. The types LINER, Seyfert and TO are aggregated and considered as the optical AGN. It is important to notice that the catalogue does not include galaxies that present broad emission lines as Seyfert 1. In practically all of the galaxies (99.9 per cent) an [O III] emission line (at 500.7-nm) with a luminosity of $10^{6.5}\,{\rm L}_\odot$ would be detectable above the noise in our sample. To obtain a complete unbiased

sample of active galaxies traced by optical emission lines, we used this cutoff for galaxies classified as optical AGN or as star forming (SF). The galaxies with [O III] luminosities below this threshold were included in the passive galaxies group.

Best & Heckman (2012) obtained the radio nuclear activity classification for galaxies in the MPA-JHU catalogue. The method followed the techniques presented in Best et al. (2005b) and used radio-continuum data from the National Radio Astronomy Observatory (NRAO) Very Large Array (VLA) Sky Survey (NVSS; Condon et al. 1998) and the Faint Images of the Radio Sky at Twenty centimetres (FIRST; Becker, White & Helfand 1995) data bases. The separation between 'low-excitation' and 'high-excitation' radio galaxies (LERG and HERG, respectively) is also given. The radio-continuum luminosity limit at $z = 0.1$, corresponding to the flux density level (5 mJy) achieved in the cross-matching process, is $L_{1.4\,\mathrm{GHz}} \approx 10^{23}$ W m^{-2} Hz^{-1}. We consider as radio AGN galaxies those that are classified as a radio AGN by Best & Heckman (2012) and have a radio luminosity above this threshold.

Table 1 shows a breakdown of the number of galaxies in each sample depending on their classification.

2.3 Potential companions

For our tidal forces estimator (see Section 3.2), when investigating potential companions for our targets we need to consider not only the SDSS spectroscopic galaxies but also galaxies with similar luminosities that were not covered by the spectroscopic survey (e.g. due to fibre allocation restrictions) and galaxies with lower luminosities (below the spectroscopic magnitude limit) that could be companions of our targets. We considered the objects in the SDSS Galaxy catalogue with: (a) r magnitude below 22.0, and (b) spectroscopic redshift below 0.11, or photometric redshift minus three times its error below 0.10. With this magnitude limit we include potential companions at least ≈50 times less luminous than the least luminous target galaxy at a given redshift. The spectroscopic redshift was used when available and the photometric redshift was considered in the other cases (whenever it was used, our methods took into account its larger relative error). Various photometric redshift catalogues have been constructed from SDSS data, and we compared these against spectroscopic redshift catalogues in different magnitude ranges to choose which to use. We selected the photometric redshift provided in the column `photozcc2` of the schema `Photoz2` (Oyaizu et al. 2008; Cunha et al. 2009) for galaxies with a magnitude fainter than 17.77 because its distribution with respect to the redshift was clearly the most accurate in the magnitude range $17.77 < r < 22.0$. For galaxies without spectra and $r < 17.77$, we used the photometric redshift provided in the column `z` of the schema `Photoz`, which seemed to agree better with spectroscopic redshifts for galaxies at these magnitudes.

3 ENVIRONMENTAL PARAMETERS

We chose three different parameters to trace different aspects of the environment and the interaction level. We defined a local density and a tidal forces estimator and obtained an estimation of group richness from the literature.

3.1 Density estimator

The density estimator (also called local density estimator) traces the density of companions around the target galaxy which is related to the dark matter halo density and is usually defined by the distance to the fifth or 10th nearest neighbour (e.g. Dressler 1980; Miller et al. 2003; Best 2004; Verley et al. 2007). It can be defined as

$$\eta_{\mathrm{t}} \equiv \log\left(\frac{k}{\mathrm{Vol}(r_k)}\right) = \log\left(\frac{3k}{4\pi r_k^3}\right),$$

where r_k is the projected distance (in Mpc) to the kth nearest neighbour. It is possible to find different definitions of this parameter in the literature. In some cases, a cylindrical volume or a surface density (e.g. Best 2004) is used. Note that the main factor that drives the parameter is the ratio k/r_k and these different definitions produce only a scaled or shifted version of η_{t}.

We dynamically obtained a list of potential companions around each of our galaxies within a given radius. We considered as companions galaxies with a difference in spectroscopic redshift lower than 0.01 ($|z_{\mathrm{c}} - z_{\mathrm{t}}| \leq 0.01$) corresponding to $\Delta v < 3000$ km s^{-1} and with luminosities in r band between $10^{9.86}$ and $10^{12.0}$ L$_\odot$. The lower limit of $10^{9.86}$ L$_\odot$ corresponds to the luminosity limit of the main spectroscopic sample at redshift 0.1. Once selected, all the potential companions were supposed to be at the same distance as the target galaxy and the k-corrections were computed using the analytical method of Chilingarian, Melchior & Zolotukhin (2010). We used the distance to the 10th nearest neighbour.

The main spectroscopic sample is ∼94 per cent complete (Strauss et al. 2002). The spatial distribution of the few galaxies with similar magnitudes that are not covered by the spectroscopic survey could affect the accuracy of the environmental estimation for some galaxies. However, given the size of the sample under study this is unlikely to be important unless it introduces systematic biases. One indicator of a systematic bias in the local density is the presence of a dependence with redshift. If the number of companions is under- or overestimated by our method for a given redshift range, a monotonic trend in the mean values of the estimator should be expected. In Fig. 1 the dependence of the local density (upper panel) with redshift is shown. There is no strong trend with redshift for the parameter. The variation of the mean with redshift is less than 0.84 per cent with respect to the variation range of the local density.

3.2 Tidal forces estimator

The tidal estimator traces the relative tidal forces exerted by companions with respect to the internal binding forces of the target galaxy (Verley et al. 2007). The definition is

$$Q_{\mathrm{t}} \equiv \log\left(\sum_i \frac{M_{\mathrm{t}}}{M_i}\left(\frac{D_{\mathrm{t}}}{d_{i,t}}\right)^3\right) = \log\left(\sum_i \frac{Lr_{\mathrm{t}}}{Lr_i}\left(\frac{2R_{\mathrm{t}}}{d_{i,t}}\right)^3\right),$$

where D is the estimated diameter of the target galaxy and R is its radius, d is the distance between the target and the companion, Lr is the corrected luminosity in r band and M is the mass of the galaxy. The luminosity in r band is used, in this case, as a proxy for the mass of the galaxy. To broadly match the definition of diameter used in the literature (projected major axis of a galaxy at the 25 mag arcsec^{-2} isophotal level or D_{25}; Verley et al. 2007), we estimated the radius by using the Petrosian radius containing 90 per cent of the total flux (r_{90}; provided in the SDSS catalogue) scaled by a factor of 1.46 (see Argudo-Fernández et al., in preparation).

For the tidal force estimator, the inclusion of the photometric galaxies (see Section 2.3) is critical, both because the SDSS fibre allocation process may not allow close companions to be targeted, and because the tidal forces are often dominated by nearby galaxies of lower luminosity. The first step before computing the tidal parameter was therefore to select which potential companions were actually associated with our target galaxy rather than

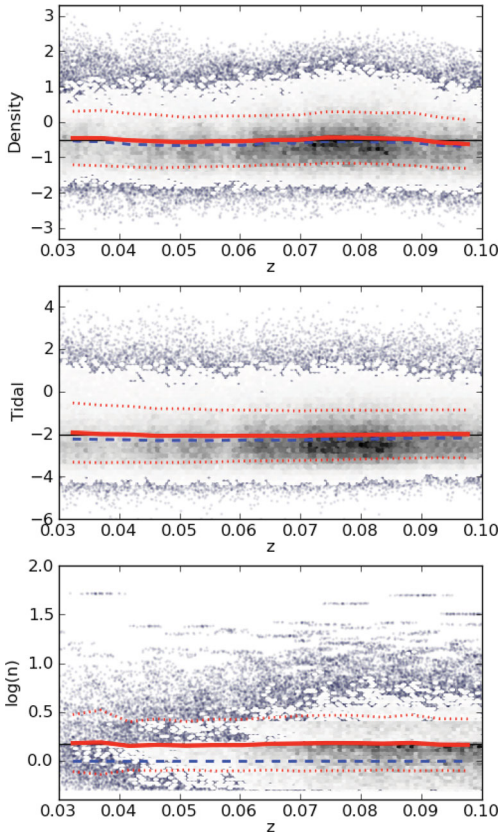

Figure 1. Dependence of the environmental parameters on the redshift. The relations of the local density (upper panel), tidal forces (middle panel) and cluster richness (lower panel) estimators with respect to the redshift are shown. The values for the target galaxies are shown as a grey-scale density cloud and dots for the outliers. 15 redshift bins were used. The mean (red solid line), its error (red dotted line) and the median (blue dashed line) for each redshift bin are plotted. The underlying black solid line marks the mean value for the whole sample. A random offset (ranging from −0.5 to 0.5) was introduced in the cluster richness parameter (n) to allow a proper visualization of the plot.

being foreground/background galaxies. For each potential companion galaxy without spectroscopy, we estimated the probability for it to be associated with the target galaxy by chance, and we used this probability to discard spurious companions. Specifically, for a hypothetical target at a redshift z, we computed the sky density of galaxies within the SDSS with an r-band magnitude brighter than a limit ($r_{\rm lim}$) and with the difference between their photometric redshift and the redshift of the target being less than N times the error of the photometric redshift. Hence, we obtained the surface density of galaxies as a function of z, $r_{\rm lim}$ and N. For each potential companion, the expected surface density of companions with its properties ($r < r_{\rm c}$, $z = z_{\rm t}$ and $N < \frac{z_{\rm p,c} - z_{\rm t}}{\Delta z_{\rm p,c}}$) was computed (the subindexes t and c denote target and companion respectively, $z_{\rm p}$ is the photometric redshift and $\Delta z_{\rm p}$ is its error). If the expected number of companions within the area defined by the distance between the companion and the target galaxy is less than 0.05, we considered the candidate galaxy as a genuine companion. Potential companions with spectroscopy were selected if $|z_{\rm c} - z_{\rm t}| \leq 0.01$. The selected companions (photometric and spectroscopic) were presumed to be at the same distance as the target galaxy and k-corrections were applied.

The search radius for tidal companions was limited to 3 h^{-1} Mpc around the target (∼4.29 Mpc using the cosmology specified in Section 1). We empirically checked that increasing the search radius above this limit produced no appreciable change in the tidal parameter. If the relative force (tidal force over internal binding force) exerted by an individual companion is defined as $q_{{\rm t},i} = (Lr_{\rm t}/Lr_i)(2R_{\rm t}/d_{i,t})^3$ such that $Q_{\rm t} = \log(\sum_i q_{{\rm t},i})$, the contribution of companions above the 3 h^{-1} Mpc limit was always $q_{{\rm t},i} \leq 10^{-6}$, while the mean for closer companions is $q_{{\rm t},i} \sim 10^{-2}$. After the rejection of spurious candidates, the tidal parameter was computed. In the rare case that no companions were selected ($N = 684$), an upper limit of $Q = -6$ was assigned to the galaxy. A galaxy ≈100 times more massive than the target would be required to produce this effect at a distance of ≈3 h^{-1} Mpc, our search radius limit.

As a test for systematic biases, the middle panel of Fig. 1 shows the dependence of the tidal forces estimator with the redshift. In this case, the variation of the mean is less than 0.37 per cent of the variation range of the parameter.

It is important to note that the tidal estimator uses the projected two-dimensional distance as the distance between the target and the companion. This will lead to a general overestimation of the tidal parameter with respect to its actual value. The overestimation can be more severe in regions with a high density of galaxies. However, as the projected distance depends only on the (random) line of sight with respect to the observer, we do not expect a systematic bias to be introduced by this effect. The expected effect is a possible decrease in the strength of the correlations between the tidal parameter and other properties, due to a degree of random scattering in the tidal paremeter measurement.

3.3 Cluster richness estimator

The last parameter is an estimation of the number of galaxies in the cluster or group to which our target galaxy belongs. Tago et al. (2010) extracted groups of galaxies from the SDSS DR7 using a modified FoF algorithm. A flux-limited sample and three volume-limited samples were provided. The groups of galaxies were detected and a value (n) was assigned to each galaxy corresponding to the number of galaxies in its own group, the cluster richness. The number density of groups detected by FoF techniques depends strongly on redshift for a flux-limited sample, hence, a volume-limited sample is required to avoid any biases. The volume-limited sample which covers all our redshift range is the DR7-20. The cut-off is $M_r - 5\log(h) = -20$ ($M_r \approx -19.2$) which covers from $z = 0.02595$ to $z = 0.11012$ given the magnitude limits of the SDSS. Therefore, in our analyses, the *reduced sample* is composed of the galaxies that are bright enough in r band and have an assigned value for the cluster richness. The value of the cluster richness ranges from 1 to 52.

The dependence of cluster richness with redshift is shown in the lower panel of Fig. 1. The variation of the mean is less than 3.16 per cent of the variation range of the parameter. The presence of a few clusters with a high number of galaxies causes this slightly higher value with respect to the other parameters. The low values found for the variance of the mean of the three environmental parameters with respect to the redshift make us consider that they are not biased.

3.4 Principal component analysis

The three presented parameters provide three complementary measures of the environment. The distribution of the local density and

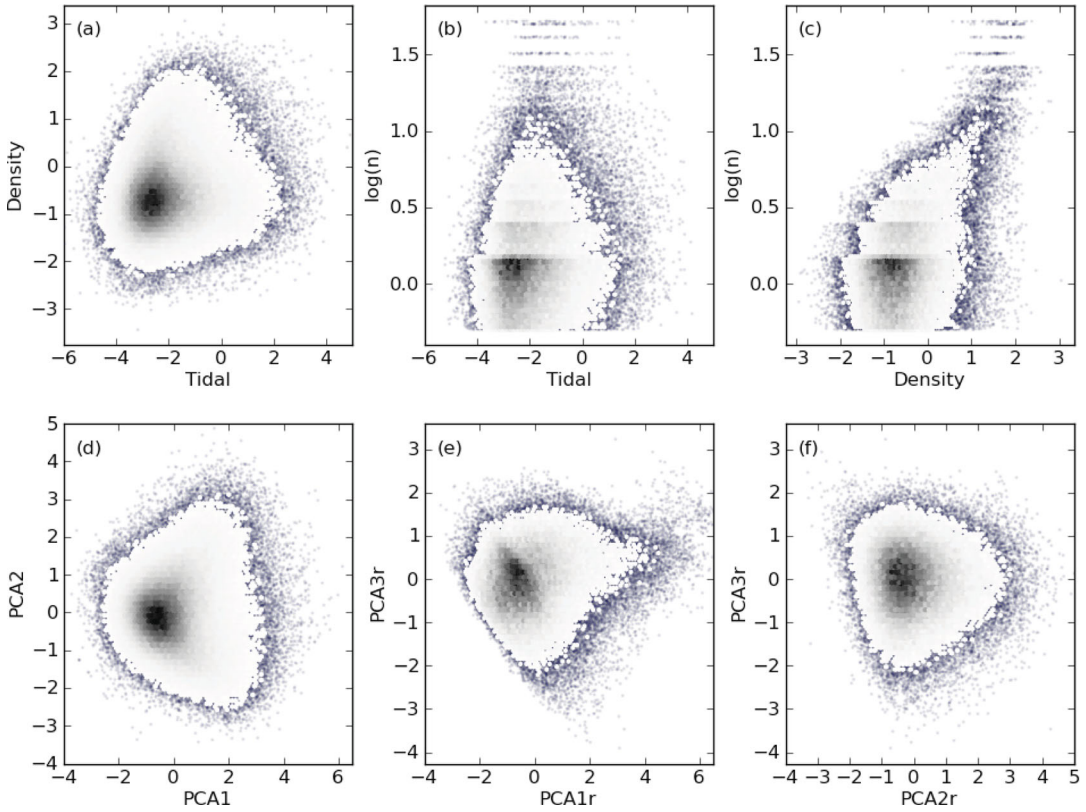

Figure 2. Environmental parameters. Panels (a) and (d) show the distribution for the whole sample and the rest of the panels for the reduced sample. The values for the target galaxies are shown as a grey-scale density cloud and dots for the outliers. A random offset (ranging from −0.5 to 0.5) was introduced in the cluster richness parameter (n) to allow a proper visualization of the plots.

the tidal forces estimator is shown in panel (a) of Fig. 2. Galaxies located at higher densities present medium to high tidal values but the highest tidal values are found for galaxies located in regions with medium to low densities. These galaxies are sometimes labelled as 'field' galaxies according to their local density but they are clearly interacting. Hence, it is important to notice that the concept 'field' and 'isolated' are not equivalent. Panels (b) and (c) of Fig. 2 show the relation of the cluster richness estimator with the local density and the tidal parameter, respectively. Each value of the cluster richness spans over a wide range of tidal and density values. In the case of the local density, it is clear that richer clusters present higher values of the local density.

We performed a Principal Component Analysis (PCA) to break the parameters down into the independent physical processes by removing the possible correlations between them. For example, part of the relation between the density and the tidal parameter was expected to be produced by projection effects, with generally higher tidal values for galaxies that are located in denser environments. Some degree of relation between the group richness and the density was also expected, as found.

We obtained two PCA components by combining the local density and the tidal parameters for the whole sample and three components for the reduced sample where we added the group richness [the suffix 'r' was added to distinguish these principal components; we entered log (n) instead of n as the input of the PCA]. The PCA components are shown in Table 2 and the normalization values applied to the environmental parameters are shown in Table 3. The effect of the two-dimensional projection on the tidal parameter was at least partially mitigated after considering the correction introduced by PCA2 with respect to the density (and cluster richness).

Table 2. PCA results.

		Density	Tidal	log(n)	*Var.*[a]
Whole	PCA1	0.707	0.707	–	57 per cent
Sample	PCA2	−0.707	0.707	–	43 per cent
Reduced	PCA1r	0.661	0.351	0.663	53 per cent
Sample	PCA2r	−0.254	0.937	−0.242	31 per cent
	PCA3r	−0.706	−0.008	0.708	16 per cent

[a]Variance carried by the PCA component.

Table 3. PCA normalization values.

	Parameter	Mean	Standard deviation
Whole	Tidal	−2.0275	1.1952
Sample	Density	−0.5082	0.7254
Reduced	Tidal	−1.8951	1.1788
Sample	Density	−0.4865	0.7100
	log(n)	0.1708	0.2748

As it is shown in Table 2, PCA1 and PCA1r are composed of a positive contribution of all the environmental parameters. PCA2 results from a positive contribution of the tidal parameter and a negative contribution of the density estimator, with PCA2r also having a negative cluster richness contribution. This similarity leads us to consider that PCA1 and PCA1r trace practically the same fundamental property, as do PCA2 and PCA2r. We later checked that the results obtained using either PCA1 and PCA2 or PCA1r and PCA2r were similar, hence, we will show the numbers obtained

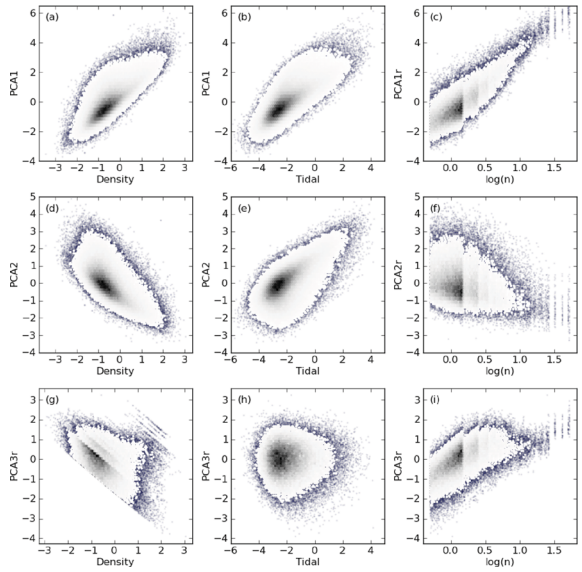

Figure 3. Relation between the environmental parameters and the PCA. Panels (a), (b), (d) and (e) show the distribution for the whole sample and the rest of the panels for the reduced sample. The values for the target galaxies are shown as a grey-scale density cloud and dots for the outliers. A random offset (ranging from −0.5 to 0.5) was introduced in the cluster richness parameter (n) to allow a proper visualization of the plots. This random offset was also propagated to the PCA components that involve the reduced sample for the same reason.

using the tidal, density, PCA1 and PCA2 for the whole sample and the cluster richness and PCA3r for the reduced sample. The relations between the PCA components are shown in Fig. 2.

We interpret the PCA components as follows.

(i) PCA1 and PCA1r follow the direction of the increase of the density (and the cluster richness) and also the tidal forces. We consider it to trace the overall interaction level and environmental nature of a galaxy.

(ii) PCA2 and PCA2r are mainly driven by the difference between the density (and cluster richness in the case of PCA2r) with respect to the tidal forces. A higher value traces higher one-on-one interactions while a lower value traces galaxies that are relatively isolated for its overall environment.

(iii) PCA3r is practically not affected by the tidal force and is driven by the difference between the density and the cluster richness. In this case, a galaxy within a rich group but with low local density values has high PCA3r values and vice versa. Hence, it would probably trace scatter in density versus cluster richness relation, being high where densities are low for that particular n (e.g. cluster outskirts) and low in particularly locally compact structure (e.g. compact groups).

In Fig. 3, the relations between the PCA components and the environmental parameters are shown. PCA parameters were computed applying the values presented in Table 2 to the normalized version of the environmental estimators obtained using the parameters presented in Table 3. The final values of the environmental estimators for all galaxies in the sample are presented in Table 4.

4 RESULTS

Our aim was to compute the relative fraction of each type of AGN with respect to the environmental and PCA parameters. The strong dependence of the prevalence of AGN with the mass of the host galaxy in the case of optical (Kauffmann et al. 2003b) and radio (Best et al. 2005a) AGN has to be considered. Hence, to begin with, we divided the sample into four bins with masses between $\log(M) = 10\,[\mathrm{M}_\odot]$ and $\log(M) = 12\,[\mathrm{M}_\odot]$ for radio AGN and six bins with masses between $\log(M) = 10\,[\mathrm{M}_\odot]$ and $\log(M) = 11.8\,[\mathrm{M}_\odot]$ for optical AGN; the AGN fractions as a function of environmental parameters are shown for each of these mass bins in Fig. 4. The monotonic increase of the fraction of active galaxies with respect to the mass of the host is clearly visible. This increase is steeper for radio AGN than for optical AGN. For radio AGN the trends of AGN fraction with environmental parameters are very similar for the four mass slices. In the case of optical AGN the trends are consistent for the density, PCA1 and PCA2 but for the tidal estimator, the cluster richness and PCA3r the results are not so clear. The bin of masses between $\log(M) = 11.5\,[\mathrm{M}_\odot]$ and $\log(M) = 11.8\,[\mathrm{M}_\odot]$ tends to not agree with the others, probably because of the low number of galaxies within this mass range (389 galaxies in the reduced sample or 432 galaxies in the whole sample which represent 0.4 or 0.2 per cent of the total number of galaxies considered, respectively).

Although the overall trends could be inferred from Fig. 4, methods that allow an aggregation of the information of the different mass slices and hence a quantitative measurement of the effect of the environmental or PCA parameter are preferable. With the aggregation, a better signal-to-noise ratio can be obtained and the quantification allows us to draw more robust conclusions. Therefore, we first defined an aggregated ratio that joins the trends found in the different slices, and then, a statistical test that takes into account the effect of the mass (as a possible confounding factor) was applied.

Table 4. Environmental parameters. The full table is available in electronic form at the CDS website http://cdsweb.u-strasbg.fr and in the online version of the journal.

Plate	mjd	FibreID	Density	Tidal	log(n)	PCA1	PCA2	PCA1r	PCA2r	PCA3r	Mass	Class.[a]
267	51 608	1	−1.318	−2.881		−1.294	0.284				9.62	--S-
286	51 999	1	−1.159	−1.904	0.000	−0.562	0.708	−1.041	0.384	0.229	10.63	--AT
291	51 928	1	−0.497	−2.878		−0.492	−0.514				10.25	----
297	51 959	1	−0.943	−2.546		−0.730	0.116				10.32	----
299	51 671	1	−0.189	−2.570	0.000	−0.010	−0.632	−0.336	−0.491	−0.731	10.77	--AS
...	...	...	...	...	...	...	...	...	...	...	...	...

[a]Classification code. The first pair of characters refers to radio activity and the second pair to optical activity. First character, radio AGN classification: R Radio AGN; - Not a radio AGN. Second character, type of radio AGN: H HERG; LLERG; - Non-classified. Third character, optical AGN classification: A optical AGN; S star forming nuclei; - Passive. Fourth character, type of optical AGN activity: S Seyfert; LLINER; T Transition object; -Not an optical AGN.

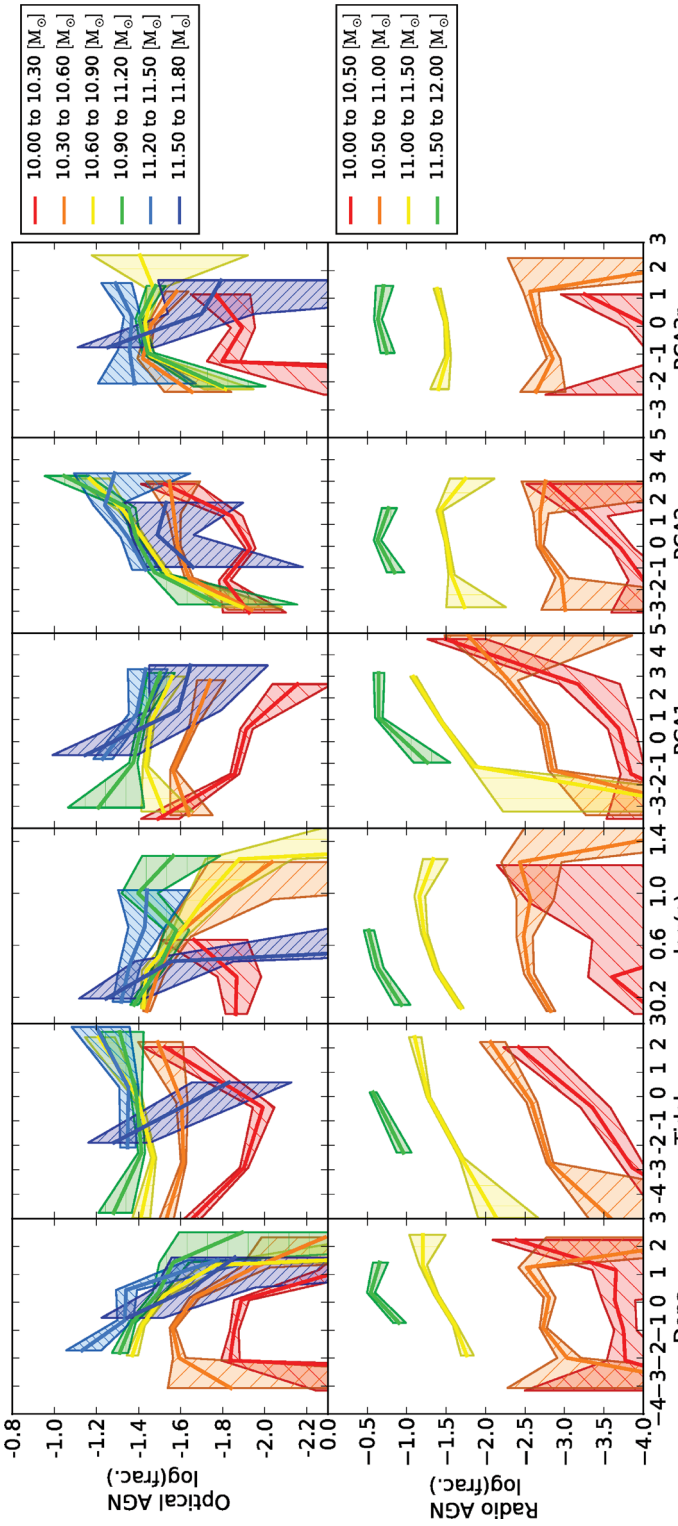

Figure 4. Fraction of optical or radio AGN galaxies, segregated in mass slices, with respect to the different environmental parameters. The bins with less than 20 galaxies (large error bars) were removed from the plots. Filled regions mark the $\pm 1\sigma$ error zone.

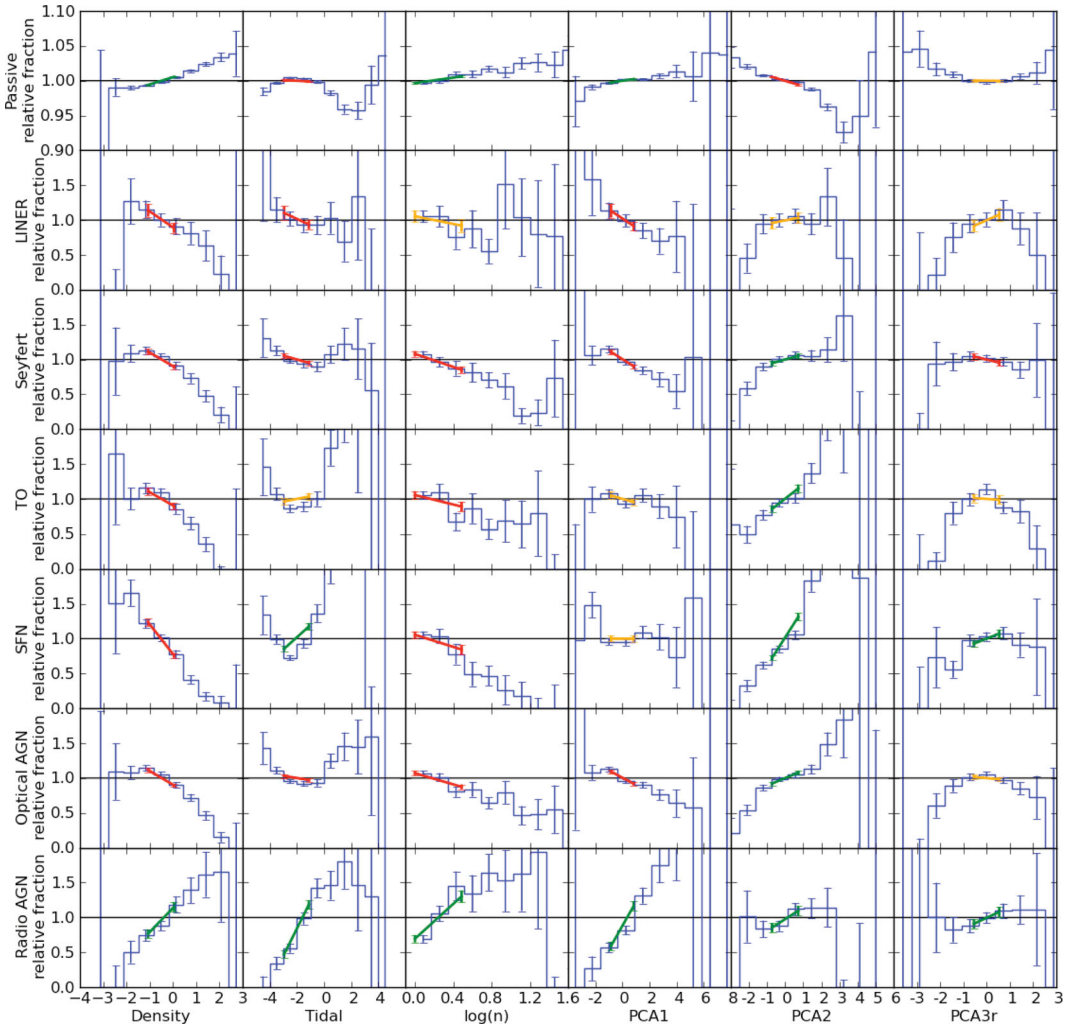

Figure 5. Relative fraction of galaxies of one type, corrected for the effect of mass, with respect to the different environmental parameters. The blue thin solid lines mark the detailed trend of f with respect to each environmental parameter. The thick solid lines defined by two points show the coarse general trend of f. The colour of the thick colour line indicates whether a flat trend is compatible within the error (orange) or not (increase – green; decrease – red).

4.1 Stratified study

To discard the effect of the mass on the fraction of AGN, we performed a stratified study of the ratio of AGN with respect to each environmental parameter. The sample was sliced in several mass strata (defined by the subindex i) and also in several bins of the environmental parameter considered (defined by the subindex j). This two-dimensional grid (i, j) was fixed, and the following values were counted for each bin: (a) $n_{i,j}$; the total number of galaxies in a bin and (b) $n_{a,i,j}$; the total number of galaxies with a given type of nuclear classification in a bin (we will use the term AGN from now on, although it can refer to any type of nuclear activity including passive galaxies). The probability of a galaxy to harbour an AGN in each mass stratum is $p_{a,i} = \sum_j n_{a,i,j} / \sum_j n_{i,j}$. If there is no environmental dependence of the AGN fraction, then an estimated value of the number of AGN in each bin of the grid can be computed as $n_{a\_\mathrm{est},i,j} = p_{a,i} n_{i,j}$. This estimate accounts for the dependence on mass, so any remaining effect is due to environment.[1] Hence, a trend of the prevalence of AGN with respect to the environmental parameter, that takes into account the effect of the mass, can be extracted by comparing $n_{a\_\mathrm{est},i,j}$ and $n_{a,i,j}$. The general trend with respect to the environmental parameter can be found by folding into the mass axis: $n_{a\_\mathrm{est},j} = \sum_i n_{a\_\mathrm{est},i,j}$, $n_{a,j} = \sum_i n_{a,i,j}$ and $n_j = \sum_i n_{i,j}$. Then, the probabilities of harbouring an AGN with respect to the environmental parameter are $p_{a,j} = n_{a,j}/n_j$ while the estimated value (taking account of the mass distribution) is $p_{a\_\mathrm{est},j} = n_{a\_\mathrm{est},j}/n_j$. The errors on these values can be calculated following a binomial distribution. The final trend, defined by the relative fraction between the observed and the estimated probabilities, is $f_i = p_{a,i}/p_{a\_\mathrm{est},i}$. A value of $f_i - \Delta f_i > 1$ or $f_i + \Delta f_i < 1$ means that, for this range of the environmental parameter, there is a significant increase/decrease of the observed fraction of AGN with respect to the expected one, after correcting for the effect of the mass.

In Fig. 5, f_i is shown for the different types of nuclear activity and environmental parameters. Seven bins were used in the mass axis and 10 bins in the environmental parameter axis defining a detailed trend. A coarse general trend using two bins is also shown. These two bins were separated at the median of each environmental or PCA parameter except in the case of the cluster richness for which galaxies with $n = 1$ were grouped in the first bin and the rest in the second one. We also divided the cluster richness in two bins using

[1] Notice that we remove largely the mass effects but small residual trends can remain if e.g. AGN and all galaxies are differently distributed within the defined mass bins.

the median after discarding galaxies with $n = 1$ and found that the trends were the same.

The trends with respect to the density are clear and monotonic. There is an increase with density in the prevalence of passive galaxies and radio AGN and a decrease for all the optical AGN types and SFN. The trends are similar for the cluster richness but slightly less acute. The tidal parameter shows a non-linear trend for optically selected types with the lowest AGN fractions at intermediate values. This may be related to correlations with other parameters. For example, the galaxies which are located in high-density regions tend to have medium tidal values [see panel (a) in Fig. 2], and the strong trends found with respect to the density might therefore affect the relative ratio for galaxies with mid-tidal values. This interpretation is supported by the fact that there is a direct clear relation between PCA2 and the presence of all types of activity; this also demonstrates the power of the PCA analysis in separating the different physical processes. The trends with respect to PCA1 are similar to the density ones but lowered, especially for galaxies which present star formation (TOs and SFN). It is noteworthy that while radio AGN and passive galaxies show the same general trend with respect to density, they show opposite trends with respect to the tidal and PCA2 parameters. The relations with respect to PCA3r are usually non-linear (see Fig. 5); these type of non-linear trends were also observed by Pimbblet et al. (2012) for the fraction of optical AGN with respect to the distance to the centre of a cluster. This non-linearity weakens the trends found using only two bins, making it difficult to draw strong conclusions. Nevertheless, some results are apparent. A lower fraction of optical AGN is generally found for lower values of PCA3r (high-density smaller systems, e.g. compact groups). There is also a possible decrease of the fraction of LINERS and TOs towards higher values of PCA3r (e.g. cluster outskirts).

4.2 Cochran–Mantel–Haenzsel test

The Cochran–Mantel–Haenzsel test (CMH; Cochran 1954; Mantel & Haenszel 1959) can be used to study the strength of the association between two bi-valued variables (odds ratio) and its significance after taking into account the effect of the possible confounding factors. In our case, we corrected for the effect of the mass. The first variable was the 'exposure' to the environmental parameter and the second variable was the effect of this exposure on the triggering of certain type of nuclear activity. We discern the 'exposure' to the environmental parameter by separating galaxies above and below the median value for a given environmental or PCA parameter. In the case of the cluster richness, more than a half of the galaxies have an assigned n of 1. Hence, the two selected groups were galaxies with $n = 1$ and galaxies with $n \geq 2$.

We tested if the prevalence of galaxies with certain type of activity is independent of the environment or interaction traced by the belonging to one of the two groups described before (galaxies with high or low values of the environmental parameter or PCA). We obtained the CMH ratio and its significance. The CMH ratio is the relative probability between the groups with high and low environmental parameters. A ratio compatible with 1 means that the prevalence of nuclear activity is independent of the environmental or PCA parameter or that a dependence cannot be found with the data used. A significant ratio (defined by the p-value), higher or lower than 1, indicates that this environmental or PCA parameter is increasing or decreasing the chance for a galaxy to harbour this type of nuclear activity.

The results of the CMH statistical test are shown in Table 5 and in Fig. 6 they are shown in a way that allows a quick visual comparison between them. We added in this case a separation of radio AGN into HERG and LERG types. An increase in the local density produces a decrease in the prevalence of optical AGN (LINER, Seyferts, TOs) and SFN. The effect is the opposite for radio AGN and passive galaxies. When we separate radio AGN in HERG and LERG, they present opposite trends with respect to the local density: LERGs show a clear increase with density while HERGs appear to show a decrease like optical AGN (though uncertainties are large due to the small sample size). The effect of the tidal parameter is not clear for passive galaxies and TOs (as expected from the non-linear

Table 5. Statistical study results from the CMH test. For each cell of the table the first row shows the CMH common odds ratio and its error and the second row shows the statistical significance or p-value (i.e. the probability of the trend occurring by chance) measured by the CMH test. The hypothesis tested was that the observed nuclear activity type is independent of the environmental or PCA parameter. The typeface of the p-value depends on its value: bold if $p < 0.01$; bold italics if $0.01 \leq p < 0.05$; regular if $0.05 \leq p < 0.1$; and italics if $p \geq 0.1$

	Density	Tidal	log(n)	PCA1	PCA2	PCA3r
Passive	1.358 ± 0.061	0.950 ± 0.043	1.248 ± 0.077	1.143 ± 0.052	0.745 ± 0.034	0.989 ± 0.055
	0.0000	***0.0296***	**0.0000**	**0.0000**	**0.0000**	*0.7025*
LINER	0.77 ± 0.11	0.84 ± 0.13	0.87 ± 0.14	0.80 ± 0.12	1.08 ± 0.16	1.18 ± 0.19
	0.0012	***0.0353***	*0.1248*	**0.0053**	*0.3375*	0.0642
Seyfert	0.801 ± 0.054	0.898 ± 0.061	0.783 ± 0.070	0.807 ± 0.055	1.118 ± 0.076	0.914 ± 0.076
	0.0000	**0.0029**	**0.0000**	**0.0000**	**0.0018**	***0.0406***
TO	0.807 ± 0.076	1.08 ± 0.10	0.84 ± 0.10	0.906 ± 0.086	1.35 ± 0.13	0.97 ± 0.11
	0.0000	*0.1568*	**0.0097**	0.0510	**0.0000**	*0.6727*
SFN	0.608 ± 0.051	1.39 ± 0.11	0.787 ± 0.100	0.999 ± 0.082	1.84 ± 0.15	1.16 ± 0.13
	0.0000	**0.0000**	**0.0005**	*0.9783*	**0.0000**	**0.0085**
Optical AGN	0.797 ± 0.042	0.939 ± 0.050	0.808 ± 0.056	0.831 ± 0.044	1.181 ± 0.062	0.964 ± 0.061
	0.0000	***0.0253***	**0.0000**	**0.0000**	**0.0000**	*0.2790*
Radio AGN	1.55 ± 0.21	2.77 ± 0.52	2.00 ± 0.28	2.13 ± 0.36	1.31 ± 0.18	1.20 ± 0.16
	0.0000	**0.0000**	**0.0000**	**0.0000**	**0.0003**	***0.0113***
LERG	1.63 ± 0.23	2.96 ± 0.59	2.07 ± 0.30	2.21 ± 0.38	1.30 ± 0.18	1.19 ± 0.16
	0.0000	**0.0000**	**0.0000**	**0.0000**	**0.0004**	***0.0185***
HERG	0.55 ± 0.27	1.01 ± 0.52	1.07 ± 0.56	1.09 ± 0.57	1.47 ± 0.75	1.81 ± 0.97
	0.0720	*0.9881*	*0.8496*	*0.8141*	*0.2897*	*0.1248*

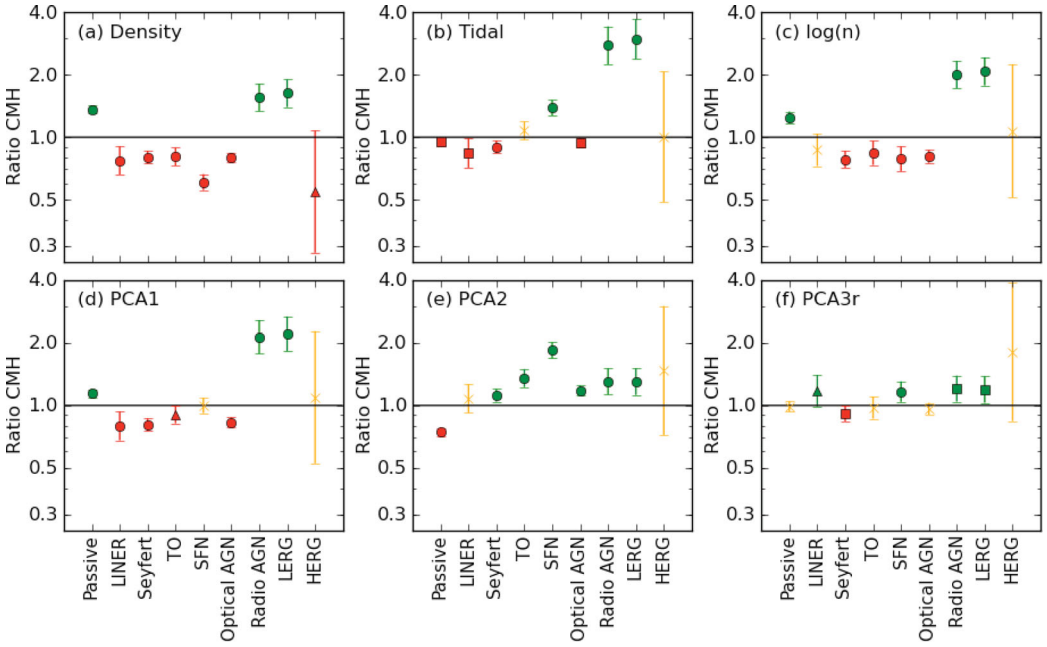

Figure 6. CMH ratios for the different types of nuclear activity with respect to the environmental parameters. The error bars mark the 95 per cent confidence interval. The shape of the symbol indicates the confidence level of the hypothesis tested (the probability of harbouring this type of activity is not affected by the environmental parameter) measured by the p-value: circle if $p < 0.01$; square if $0.01 \leq p < 0.05$; triangle if $0.05 \leq p < 0.1$; and cross if $p \geq 0.1$.

dependence in Fig. 5). A slight decrease of the fraction of LINERs and Seyferts with increasing tidal parameter is found while an increase is found for SFN and radio AGN. This might be caused by the non-linear relation due to the effect of high-density galaxies explained before. The trends with respect to the cluster richness are similar to the trends with density. The effects that depend on PCA1 are very similar to the ones driven by density except for SFN. Probably the decreasing prevalence of SFN with density is compensated by the increasing prevalence with the tidal estimator to make the PCA1 relation flat. In the case of increasing PCA2, there is an increase in the AGN fraction for Seyferts, TOs, SFN and radio AGN and a clear decrease for passive galaxies. The trends for HERGs and LERGs are compatible here. PCA2 reveals much stronger positive trends for optical AGN than tidal does, due to removal of density selection effects, i.e. using PCA we show the importance of the one-on-one interactions. The radio AGN trend with PCA2 is much weaker than that with the tidal parameter, indicating that much of what is seen with respect to the tidal parameter is just a density effect (which gets stronger going from density to PCA1). The trends with PCA3r generally tend to be weaker and more variable for optical AGN types, as expected from the non-linearities shown in Fig. 5. However, radio AGN and SFN have clearly increasing fractions with an increasing PCA3r.

5 DISCUSSION

5.1 Environment and interactions

Of the parameters studied, mass is confirmed to be the main driving factor for the triggering of an AGN, especially for radio AGN (Kauffmann et al. 2004; Best et al. 2005a) as shown in Fig 4. However, both local density and interactions also play a significant role in the prevalence of nuclear activity. Fig. 6 and Table 5 show the clear relations between the prevalence of the different types of nuclear activity with the environmental parameters. The relations obtained show the clearly different and even opposite trends found for the AGN fraction depending on the environmental or PCA parameter used and the type of AGN studied. These differences may have led to previous discrepancies found in the literature.

The fraction of optical AGN decreases towards higher values of the local density, PCA1 and the cluster richness, with the prevalence of AGN in the densest local environments being a factor of 2–3 lower (at a fixed mass) than that in sparser environments. The similarity between the trends with respect to local density and cluster richness reflects that both parameters are closely related, as shown in panel (c) of Fig. 2, with galaxies with higher n located at higher densities. In rich environments there are several mechanisms that can remove or change the properties of the cold gas needed to fuel the star formation or AGN from galaxies: the stripping of diffuse gas around galaxies or strangulation, ram-pressure stripping and galaxy harassment (see von der Linden et al. 2010, and references therein). The stripping of cold gas and its warming can explain the decrease of the prevalence of optical activity (AGN and star formation) found in denser and richer environments.

On the other hand, one-on-one interactions, traced by PCA2, produce an enhancement on the prevalence of SFN, TOs, Seyfert and radio AGN and a decrease of the fraction of passive galaxies. This agrees with a scenario where galaxy interactions can fuel gas to the central region of the galaxy (Shlosman et al. 1990; Barnes & Hernquist 1991; Haan et al. 2009; Liu et al. 2011). However, notice that this is not the only mechanism that triggers nuclear activity (e.g. Silverman et al. 2011; Sabater et al. 2012); the AGN prevalence only increases by a factor of ∼2 between galaxies with no nearby neighbours to those undergoing the strongest interactions. For optically selected nuclear activity, the values of the CMH ratios with respect to PCA2 [see panel (e) in Fig. 6] decrease in this order: SFN, TOs, Seyfert, LINERs and passive galaxies. This relation can be compatible with the existence of a time delay between the tidal interaction and the setting of the different types of activity with an interaction inducing first star formation, then a Seyfert-like AGN,

and then a LINER, before returning to a passive state (e.g. Li et al. 2008; Darg et al. 2010; Wild, Heckman & Charlot 2010).

The slightly decreasing trend of AGN prevalence found for optical AGN (both LINERs and Seyferts) with respect to the tidal parameter [see panel (b) in Fig. 6] may be produced by an overestimation of the tidal parameter in regions with high density of galaxies due to the use of projected distances (as discussed earlier). Another explanation is that galaxies with a high tidal parameter located in dense environments lack the supply of gas required to fuel their nuclear activity despite their ongoing one-on-one interaction (see the next section). When this effect is corrected for using the correlation found with the PCA by the use of PCA2, the increase of the prevalence of all types of active galaxies with PCA2 becomes conspicuous. This suggests that PCA2 may trace better one-on-one interactions than the uncorrected tidal estimator, or at least, it may better trace the sort of one-on-one interactions that can trigger nuclear activity (i.e. those that fuel gas into the nucleus).

Interactions and environmental density are complementary factors that must be taken into account to get a complete view of the external phenomena that affect the triggering of an AGN. The trends found can be explained if the different parameters trace different physical processes that affect the triggering of nuclear activity.

5.2 AGN types

Optical AGN and HERG are thought to be fuelled in different ways than the prevalent population of radio AGN (LERG; Best & Heckman 2012). The first type of AGN are fuelled at relatively high Eddington rates in radiatively efficient accretion discs while the second type is fuelled at relatively low Eddington rates in radiatively inefficient accreting flows. While the first type requires a plentiful supply of cold gas, the lower accretion-rate requirements of the LERGs could be achieved by accreting warm gas located in the haloes surrounding the galaxy, cluster or group.

The local density parameter can trace the content and physical condition of the gas. The lack of cold gas in clusters of galaxies in the local Universe is well known (e.g. Giovanelli & Haynes 1985), and the gas that can be found at higher densities is warmer (see Cattaneo et al. 2009). If a plentiful supply of cold gas is required to fuel optical AGN and SFN, then these types of activity will be suppressed in dense environments but enhanced by one-on-one interactions, as discussed above. On the other hand, the accretion of warm gas would explain the higher prevalence of radio AGN of LERG type in denser environments. The result that LERGs are enhanced by one-on-one interactions, however, argues against the simplest models in which all LERGs are fuelled from the warm gas haloes around massive galaxies, groups or clusters (e.g. Hardcastle et al. 2007). It suggests that some LERGs are fuelled by other mechanisms, and supports arguments that the distinction between radiatively efficient and radiatively inefficient AGN is more likely to be a function of Eddington-scaled accretion rate (e.g. Merloni & Heinz 2008; Best & Heckman 2012) than the origin of the fuelling gas. In this picture, most galaxy interactions provide gas to the nucleus at a sufficiently high rate that a radiatively efficient (optical) AGN is produced, but in some interactions (or at some times during an interaction) the gas flow to the nucleus is slower and results in a LERG. These LERGs may be distinguishable from the cooling-fuelled LERGs in terms of their colours (e.g. Janssen et al. 2012).

The low numbers of HERGs make it difficult to draw statistically significant results from them, but their prevalence is statistically higher at lower than at higher local densities [see panel (a) in Fig. 6]. This is opposite to the trend found for LERGs but the same as that for optical AGN. Indeed, all the environmental trends for HERGs are more similar to optical AGN than to the rest of radio AGN (LERGs). This suggests that the physical processes that trigger HERGs are similar to that of optical AGN. Despite the similar powering mechanisms and environment trends, it is important to note that HERGs do show significant differences with respect to Seyferts, most particularly that they are preferentially found at higher stellar masses (median values for the whole sample: $10^{10.88}$ versus $10^{10.56}$ $M_{\odot}$; reduced sample: $10^{10.95}$ versus $10^{10.74}$ $M_{\odot}$).

The mechanisms that power LINER galaxies are a matter of controversy (Kewley et al. 2006). Some LINERs are certainly powered by accretion (e.g. González-Martín et al. 2006), but there are strong arguments that a fraction of them could be powered by low-mass evolved stars (e.g. Cid Fernandes et al. 2011). In our analysis we found that the LINERs show very similar trends to those of the rest of the optical AGN population (although some differences can be observed in PCA3r). This may be caused by the limiting luminosity that we apply to $L_{[\mathrm{O\,III}]}$, which will select only the most luminous LINERs which are more likely to be powered by AGN (Cid Fernandes et al. 2011); these may behave differently from low-luminosity AGN (Schawinski et al. 2010). This may cause the trends of our LINERs to be similar in general to those of Seyfert galaxies.

5.3 Further considerations

In Sabater et al. (2012), no evidence of a difference was found between the prevalence of AGN in isolated galaxies (AMIGA (Analysis of the interstellar Medium in Isolated GAlaxies) sample of isolated galaxies; Verdes-Montenegro et al. 2005) or in a sample of compact groups (Martínez et al. 2010) at a fixed stellar mass and morphology. This result can be explained if the increment expected in compact groups due to higher one-on-one interactions is broadly compensated by their higher local density and deficiency of cold gas (Verdes-Montenegro et al. 2001). However, an interpretation of the differences found for star formation in the literature (e.g. Sulentic et al. 2001; Durbala et al. 2008; Martinez-Badenes et al. 2012) is not straightforward.

There are additional considerations that could be taken into account to further advance this study. First, morphology could play an important role on nuclear activity (Hwang et al. 2012), and its effect as a confounding factor could also be estimated. Secondly, lower emission line luminosity systems could be probed to investigate the more typical LINER population. To allow the discrimination between genuine AGN-powered LINERs and retired galaxies whose emission resembles that of weak AGN, alternative diagnostic methods that take into account the differences between these types of weak AGN would have to be considered (Buttiglione et al. 2010; Cid Fernandes et al. 2011; Sabater et al. 2012). Thirdly, it could be investigated whether different sub-populations of LERGs (e.g. by colour or luminosity) show the same environmental and interaction dependencies. This study will be extended in the future to clarify those points.

6 SUMMARY AND CONCLUSIONS

We presented a study of the prevalence of optical and radio nuclear activity with respect to the environment and interactions in a sample of SDSS galaxies. We aimed to determine the effect of these external factors on the triggering of nuclear activity but taking into account the effect of possible confounding factors like the galaxy mass.

The study is based on a sample of ∼270 000 galaxies with a redshift between 0.03 and 0.1 drawn from the main spectroscopic

sample of the SDSS. Additional data like the stellar mass and the optical AGN classification were obtained from the MPA-JHU catalogue. The radio AGN classification is described in Best & Heckman (2012). We defined a local density parameter and a tidal forces estimator and used a cluster richness estimator from the literature (Tago et al. 2010) to trace different aspects of environment and interaction. A PCA was applied to the environmental parameters to consider and remove the possible correlations between them. A stratified statistical study, which removed the effect of the galaxy mass, was applied in order to find the unbiased relation of the prevalence of the different types of nuclear activity with the different PCA and environmental parameters. The relations were quantified and their statistical significance obtained using the CMH test.

From this study we found the following.

(i) There is a strong dependence of the prevalence of nuclear activity with density and interactions after taking into account the effect of mass. However, it is fundamental to distinguish and consider both local environment and one-on-one interactions because they can produce different and even opposite effects.

(ii) We found a decrease of optical nuclear activity, including star formation, towards denser environments. This effect is probably driven by the lack of a cold gas supply at higher densities.

(iii) On the other hand, an increase of the prevalence of radio nuclear activity is found towards higher densities. This can be explained by the warmer gas present at higher densities that is accreted at low rates in a radiatively inefficient manner, triggering *typical* low-luminosity radio AGN or LERGs.

(iv) There is an increase of the prevalence of SFN, optical and radio AGN with one-on-one interactions. The dependence for the different types of optical activity with respect to PCA2 traced by the CMH ratio follows this order: SFN (1.84), TOs (1.35), Seyferts (1.12), LINERs (1.08) and, finally, passive galaxies (0.75); this is in accordance with the time sequence that has been argued for the different activity types.

(v) The trend for HERGs with local density is statistically different to that of the rest of radio AGN (LERG) and similar to that of optical AGN. This adds evidence to the link of HERG with high excitation AGN, like optical and X-ray AGN, that needs a supply of cold gas to be powered.

Our results agree with a scenario where the type of AGN triggered is related to the presence and physical condition of the gas supply of the AGN, which in turn depends on both large-scale environment and local interactions. High excitation AGN (optical AGN and HERGs) and SFN require the presence of a plentiful cold gas supply to the nuclear regions. This gas is less likely to be present in denser environments where galaxies tend to be gas poor due to stripping or harassment. The prevalence of AGN is enhanced in the presence of one-on-one interactions which can funnel gas to the nuclear regions. These two effects may work in competition against each other (one-on-one interactions are more likely in denser environments) and hence, the consideration of different aspects of the environment is fundamental to obtain a complete understanding of the mechanisms that may trigger the different types of AGN. In contrast, low-luminosity radio AGN of LERG type require relatively low gas accretion rates. This can be supplied by the cooling of gas from the hot haloes of groups and clusters accounting for the strong increase in the prevalence of LERGs with local density. However, the presence of a residual trend with one-on-one interactions after density effects are removed (PCA2) suggests that warm gas cooling is not the only mechanism by which LERGs can be triggered.

ACKNOWLEDGMENTS

We acknowledge the useful comments of the anonymous referee. JS and MAF were partially supported by Grant AYA2011-30491-C02-01, co-financed by MICINN and FEDER funds, and the Junta de Andalucía (Spain) grants P08-FQM-4205 and TIC-114. Funding for the SDSS and SDSS-II has been provided by the Alfred P. Sloan Foundation, the Participating Institutions, the National Science Foundation, the U.S. Department of Energy, the National Aeronautics and Space Administration, the Japanese Monbukagakusho, the Max Planck Society and the Higher Education Funding Council for England. The SDSS Web Site is http://www.sdss.org/. The SDSS is managed by the Astrophysical Research Consortium for the Participating Institutions. The Participating Institutions are the American Museum of Natural History, Astrophysical Institute Potsdam, University of Basel, University of Cambridge, Case Western Reserve University, University of Chicago, Drexel University, Fermilab, the Institute for Advanced Study, the Japan Participation Group, Johns Hopkins University, the Joint Institute for Nuclear Astrophysics, the Kavli Institute for Particle Astrophysics and Cosmology, the Korean Scientist Group, the Chinese Academy of Sciences (LAMOST), Los Alamos National Laboratory, the Max-Planck-Institute for Astronomy (MPIA), the Max-Planck-Institute for Astrophysics (MPA), New Mexico State University, Ohio State University, University of Pittsburgh, University of Portsmouth, Princeton University, the United States Naval Observatory and the University of Washington.

REFERENCES

Abazajian K. N. et al., 2009, ApJS, 182, 543
Alonso M. S., Lambas D. G., Tissera P., Coldwell G., 2007, MNRAS, 375, 1017
Alonso S., Coldwell G., Garcia Lambas D., 2012, preprint (arXiv:1211.5156
Bahcall J. N., Kirhakos S., Saxe D. H., Schneider D. P., 1997, ApJ, 479, 642
Baldwin J. A., Phillips M. M., Terlevich R., 1981, PASP, 93, 5
Barnes J. E., Hernquist L. E., 1991, ApJ, 370, L65
Becker R. H., White R. L., Helfand D. J., 1995, ApJ, 450, 559
Bessiere P., Tadhunter C. N., Ramos Almeida C., Villar-Martin M., 2012, MNRAS, 426, 276
Best P. N., 2004, MNRAS, 351, 70
Best P. N., Heckman T. M., 2012, MNRAS, 421, 1569
Best P. N., Kauffmann G., Heckman T. M., Brinchmann J., Charlot S., Ivezić Ž., White S. D. M., 2005a, MNRAS, 362, 25
Best P. N., Kauffmann G., Heckman T. M., Ivezić Ž., 2005b, MNRAS, 362, 9
Best P. N., von der Linden A., Kauffmann G., Heckman T. M., Kaiser C. R., 2007, MNRAS, 379, 894
Blanton M. R., Moustakas J., 2009, ARA&A, 47, 159
Blanton M. R., Eisenstein D., Hogg D. W., Schlegel D. J., Brinkmann J., 2005a, ApJ, 629, 143
Blanton M. R. et al., 2005b, AJ, 129, 2562
Brinchmann J., Charlot S., Heckman T. M., Kauffmann G., Tremonti C., White S. D. M., 2004, preprint (arXiv:astro-ph/0406220)
Bushouse H. A., 1986, AJ, 91, 255
Buttiglione S., Capetti A., Celotti A., Axon D. J., Chiaberge M., Macchetto F. D., Sparks W. B., 2010, A&A, 509, A6
Carter B. J., Fabricant D. G., Geller M. J., Kurtz M. J., McLean B., 2001, ApJ, 559, 606
Cattaneo A. et al., 2009, Nat, 460, 213
Chilingarian I. V., Melchior A. L., Zolotukhin I. Y., 2010, MNRAS, 405, 1409
Cid Fernandes R., Stasińska G., Mateus A., Vale Asari N., 2011, MNRAS, 413, 1687
Cochran W. G., 1954, Biometrics, 10, 417
Comerford J. M. et al., 2009, ApJ, 698, 956

Condon J. J., Cotton W. D., Greisen E. W., Yin Q. F., Perley R. A., Taylor G. B., Broderick J. J., 1998, AJ, 115, 1693
Constantin A., Vogeley M. S., 2006, ApJ, 650, 727
Cunha C. E., Lima M., Oyaizu H., Frieman J., Lin H., 2009, MNRAS, 396, 2379
Darg D. W. et al., 2010, MNRAS, 401, 1552
Deng X. F., He J. Z., Wen X. Q., 2009, ApJ, 693, L71
Deng X. F., Chen Y. Q., Jiang P., 2011, MNRAS, 417, 453
Domingue D. L., Sulentic J. W., Durbala A., 2005, AJ, 129, 2579
Dressler A., 1980, ApJ, 236, 351
Durbala A. et al., 2008, AJ, 135, 130
Ellison S. L., Patton D. R., Simard L., McConnachie A. W., 2008, AJ, 135, 1877
Ellison S. L., Patton D. R., Mendel J. T., Scudder J. M., 2011, MNRAS, 418, 2043
Elvis M. et al., 1994, ApJS, 95, 1
Ferrarese L., Merritt D., 2000, ApJ, 539, L9
Gabor J. M. et al., 2009, ApJ, 691, 705
Gebhardt K. et al., 2000, ApJ, 539, L13
Georgakakis A. et al., 2009, MNRAS, 397, 623
Giovanelli R., Haynes M. P., 1985, ApJ, 292, 404
González-Martín O., Masegosa J., Márquez I., Guerrero M. A., Dultzin-Hacyan D., 2006, A&A, 460, 45
Grogin N. A. et al., 2005, ApJ, 627, L97
Haan S., Schinnerer E., Emsellem E., García-Burillo S., Combes F., Mundell C. G., Rix H. W., 2009, ApJ, 692, 1623
Hardcastle M. J., Evans D. A., Croston J. H., 2007, MNRAS, 376, 1849
Heckman T. M., 1980, A&A, 87, 152
Heckman T. M., Smith E. P., Baum S. A., van Breugel W. J. M., Miley G. K., Illingworth G. D., Bothun G. D., Balick B., 1986, ApJ, 311, 526
Hlavacek-Larrondo J., Fabian A. C., Edge A. C., Ebeling H., Allen S. W., Sanders J. S., Taylor G. B., 2012, preprint (arXiv:1211.5606)
Ho L. C., 2008, ARA&A, 46, 475
Hutchings J. B., Campbell B., 1983, Nat, 303, 584
Hwang H. S., Park C., Elbaz D., Choi Y. Y., 2012, A&A, 538, A15
Janssen R. M. J., Röttgering H. J. A., Best P. N., Brinchmann J., 2012, A&A, 541, A62
Kauffmann G. et al., 2003a, MNRAS, 341, 33
Kauffmann G. et al., 2003b, MNRAS, 346, 1055
Kauffmann G., White S. D. M., Heckman T. M., Ménard B., Brinchmann J., Charlot S., Tremonti C., Brinkmann J., 2004, MNRAS, 353, 713
Kewley L. J., Groves B., Kauffmann G., Heckman T., 2006, MNRAS, 372, 961
Koss M., Mushotzky R., Veilleux S., Winter L., 2010, ApJ, 716, L125
Koulouridis E., Plionis M., Chavushyan V., Dultzin-Hacyan D., Krongold Y., Goudis C., 2006, ApJ, 639, 37
Kuo C. Y., Lim J., Tang Y. W., Ho P. T. P., 2008, ApJ, 679, 1047
Letawe Y., Letawe G., Magain P., 2010, MNRAS, 403, 2088
Li C., Kauffmann G., Heckman T. M., White S. D. M., Jing Y. P., 2008, MNRAS, 385, 1915
Liu X., Shen Y., Strauss M. A., Hao L., 2011, ApJ, 737, 101
Liu X., Shen Y., Strauss M. A., 2012, ApJ, 745, 94
Mantel N., Haenszel W., 1959, J. Natl. Cancer Inst., 22, 719
Marconi A., Hunt L. K., 2003, ApJ, 589, L21
Martínez M. A., Del Olmo A., Coziol R., Perea J., 2010, AJ, 139, 1199
Martinez-Badenes V., Lisenfeld U., Espada D., Verdes-Montenegro L., García-Burillo S., Leon S., Sulentic J., Yun M. S., 2012, A&A, 540, A96
Martini P., Kelson D. D., Mulchaey J. S., Trager S. C., 2002, ApJ, 576, L109
Merloni A., Heinz S., 2008, MNRAS, 388, 1011
Miller C. J., Nichol R. C., Gómez P. L., Hopkins A. M., Bernardi M., 2003, ApJ, 597, 142
Moles M., Marquez I., Perez E., 1995, ApJ, 438, 604
Oyaizu H., Lima M., Cunha C. E., Lin H., Frieman J., Sheldon E. S., 2008, ApJ, 674, 768
Park C., Choi Y. Y., 2009, ApJ, 691, 1828
Petrosian A. R., 1982, Astrofizika, 18, 548
Pierce C. M. et al., 2007, ApJ, 660, L19
Pimbblet K. A., Shabala S. S., Haines C. P., Fraser-McKelvie A., Floyd D. J. E., 2013, MNRAS, 429, 1827
Ramos Almeida C. et al., 2012, MNRAS, 419, 687
Reviglio P., Helfand D. J., 2006, ApJ, 650, 717
Rogers B., Ferreras I., Kaviraj S., Pasquali A., Sarzi M., 2009, MNRAS, 399, 2172
Ruderman J. T., Ebeling H., 2005, ApJ, 623, L81
Sabater J., Leon S., Verdes-Montenegro L., Lisenfeld U., Sulentic J., Verley S., 2008, A&A, 486, 73
Sabater J., Leon S., Verdes-Montenegro L., Lisenfeld U., Sulentic J., Verley S., 2010, in Verdes-Montenegro L., Del Olmo A., Sulentic J., eds, ASP Conf. Ser. Vol. 421, Galaxies in Isolation: Exploring Nature Versus Nurture. Astron. Soc. Pac., San Francisco, p. 57
Sabater J., Verdes-Montenegro L., Leon S., Best P., Sulentic J., 2012, A&A, 545, A15
Sanders D. B., Soifer B. T., Elias J. H., Neugebauer G., Matthews K., 1988, ApJ, 328, L35
Schawinski K., Dowlin N., Thomas D., Urry C. M., Edmondson E., 2010, ApJ, 714, L108
Schmitt H. R., 2001, AJ, 122, 2243
Serber W., Bahcall N., Ménard B., Richards G., 2006, ApJ, 643, 68
Shlosman I., Begelman M. C., Frank J., 1990, Nat, 345, 679
Sijacki D., Springel V., Di Matteo T., Hernquist L., 2007, MNRAS, 380, 877
Silverman J. D. et al., 2009, ApJ, 695, 171
Silverman J. D. et al., 2011, ApJ, 743, 2
Slavcheva-Mihova L., Mihov B., 2011, A&A, 526, A43
Smirnova A. A., Moiseev A. V., Afanasiev V. L., 2010, MNRAS, 408, 400
Strauss M. A. et al., 2002, AJ, 124, 1810
Sulentic J. W., Rosado M., Dultzin-Hacyan D., Verdes-Montenegro L., Trinchieri G., Xu C., Pietsch W., 2001, AJ, 122, 2993
Tago E., Saar E., Tempel E., Einasto J., Einasto M., Nurmi P., Heinämäki P., 2010, A&A, 514, A102
Tal T., van Dokkum P. G., Nelan J., Bezanson R., 2009, AJ, 138, 1417
Tang Y. W., Kuo C. Y., Lim J., Ho P. T. P., 2008, ApJ, 679, 1094
Tasse C., Röttgering H., Best P. N., 2011, A&A, 525, A127
Taylor M. B., 2005, in Shopbell P., Britton M., Ebert R., eds, ASP Conf. Ser. Vol. 347, Astronomical Data Analysis Software and Systems XIV, Astron. Soc. Pac., San Francisco, p. 29
Urrutia T., Lacy M., Becker R. H., 2008, ApJ, 674, 80
Verdes-Montenegro L., Yun M. S., Williams B. A., Huchtmeier W. K., Del Olmo A., Perea J., 2001, A&A, 377, 812
Verdes-Montenegro L., Sulentic J., Lisenfeld U., Leon S., Espada D., Garcia E., Sabater J., Verley S., 2005, A&A, 436, 443
Verley S. et al., 2007, A&A, 472, 121
Villar-Martín M., Tadhunter C., Humphrey A., Encina R. F., Delgado R. G., Torres M. P., Martínez-Sansigre A., 2011, MNRAS, 416, 262
Villar-Martín M., Cabrera Lavers A., Bessiere P., Tadhunter C., Rose M., de Breuck C., 2012, MNRAS, 423, 80
von der Linden A., Wild V., Kauffmann G., White S. D. M., Weinmann S., 2010, MNRAS, 404, 1231
Waskett T. J., Eales S. A., Gear W. K., McCracken H. J., Lilly S., Brodwin M., 2005, MNRAS, 363, 801
Wild V., Heckman T., Charlot S., 2010, MNRAS, 405, 933
York D. G. et al., 2000, AJ, 120, 1579

SUPPORTING INFORMATION

Additional Supporting Information may be found in the online version of this article:

Table 4. Environmental parameters. (http://www.mnras.oxfordjournals.org/lookup/suppl/doi:10.1093/mnras/sts675/-/DC1).

Please note: Oxford University Press are not responsible for the content or functionality of any supporting materials supplied by the authors. Any queries (other than missing material) should be directed to the corresponding author for the article.

This paper has been typeset from a TEX/LATEX file prepared by the author.